UCID--19661

DE83 006133

Final Report
NASA Contract #NAS8-33699 & Order #H549408

Prepared for
National Aeronautics and Space Administration
George C. Marshall Space Flight Center
Marshall Space Flight Center
Alabama, 35812

by

Gregory M. Sanger
Optics Laboratory
Lawrence Livermore National Laboratory
P. O. Box 808, L-432
Livermore, California 94550

15 January 1983

LEGIBILITY NOTICE

A major purpose of the Technical Information Center is to provide the broadest dissemination possible of information contained in DOE's Research and Development Reports to business, industry, the academic community, and federal, state and local governments.

Although large portions of this report are not reproducible, it is being made available in paper copy to facilitate the availability of those parts of the document which are legible.

Introduction

This is to be considered as the final report on Contract #NAS8-33699 between the George C. Marshall Space Flight Center (NASA) and Lawrence Livermore National Laboratory. The objective of this program has been to provide NASA with general engineering support and advanced development efforts toward the construction of the optical surfaces for the Advanced X-ray Astrophysical Facility (AXAF). AXAF is a long-life high-performance, imaging X-ray observatory planned for shuttle-launched orbital flight late in the 1980's. Specific tasks planned and carried out during the period of performance (from 24 June 1980 to 31 December 1982) were:

A. Analysis and review of the applicability of precision machining technology to the manufacture of the AXAF objective mirrors;

B. Review of the proposed and alternative methods for manufacturing and testing: 1) the AXAF technology mirrors and 2) the AXAF high resolution mirror assembly;

C. Analysis, review and engineering support to NASA in the areas of surface shape and smoothness metrology for grazing incidence X-ray surfaces;

D. Determination, through analytical and experimental efforts, of the feasibility of applying heterodyne surface profilometry to non-flat surfaces; and

E. Three sets of scattering flats with known surface profiles and microtopographic character produced by precision machining and polished precision machine surfaces.

This project was contractually divided into two major task headings, "Precision Machining Technology" and "Precision Metrology for AXAF". The first covers task items A and E above and the second contains the remainder.

Task I - Precision Machining Technology

Analysis and review of the applicability of precision machining technology to the manufacture of AXAF objective mirrors. - - Our efforts to show the applicability of precision machining to X-ray optical surfaces have taken the form of reviews of proposed techniques at NASA-SAO technical reviews of contractors, manufacture of several sets of scattering flats by diamond turning for Marshall's long path X-ray scatterometer, and an assessment of the work previously carried out by Livermore in manufacturing X-ray telescopes for the University of California's Berkeley Space Sciences Program.

Members of the Livermore technical staff (J. B. Bryan and G. M. Sanger) attended several technology reviews in Huntsville and at potential vendor sites during the course of this work. Here, we served as technical advisors to NASA and SAO in their efforts to judge the viability of the processes and instruments being proposed. Specific recommendations were passed to NASA and SAO verbally. In addition, presentations on alternative processes that are applicable to AXAF manufacture were given which detailed manufacturing processes as:

a. precision machining as a roughing process;
b. precision glass grinding and glass machining;
c. polishing diamond turned components;
and test surfaces by instruments as:
(1) heterodyne optical profilometry for microtopography;
(2) holographic non-conjugate interferometry.

Lawrence Livermore has delivered six sets of scattering flats to Huntsville for evaluation in the long path vacuum scatterometer. The goal for NASA was to acquire data on the X-ray scattering properties of precision machined and polished precision machined surfaces.

The first four sets of samples were fabricated from 6061-T6 aluminum and nickel coated with ~200 μm of electroless nickel or tin nickel. The coated nickel was machined on a Pneumo Precision facing machine operated as a flycutting machine. This precision machined surface was subsequently polished for a figure of $\lambda/10$ to $\lambda/16$ (λ = 0.6328 μm) and typical finish values for metal (roughness on the order of 20-40Å RMS). Polishing was accomplished utilizing a diamond impregnated pitch technique. Here, the diamond polishing powder (1 μm to 3μm RMS particle size) was mixed with melted pitch and poured onto a preformed pure wood rosin (Gugholz #73 and #84) pitch lap. These laps were run on the samples in a silicone oil where the oil slowly dissolves the pitch away and continually exposes new polishing particles to the surface being polished. By relatively slow motions (<10 cm/sec) between the lap and workpiece and low pressures (<35 grams/cm^2), high quality surfaces (~10-30Å/RMS) may be achieved in nickel alloys.

The ULE samples were included as part of an ongoing project to determine if a relatively thick coating of a diamond turnable metal could be adherently coated onto a glass substrate without stress. This project was successful with a pure copper coating on two scattering sample sets delivered in December of 1982. The key to this technique is preparation of the glass substrate and plating at the temperature the finished component will experience during its operational life. The ULE substrates were prepared by first fine grinding the surfaces to be coated with 3 μm, RMS particle size aluminum oxide followed by an acid etch in a 6% solution HNO_3 at 100°C. The prepared surface is vacuum coated with 500-800Å of either a chromium or titanium binder layer. These metals adhere well to glass and are thin enough that the stresses are small. The final copper coating is electrodeposited at the operational temperature to a thickness that can be precision machined and polished. Such a technique may well be worth consideration in exploring alternatives to the current manufacturing techniques for the AXAF objective. The advantage would be appreciated in the significant reduction in processing time and ultimately cost of producing these optical elements.

The previous precision machining work, carried out by Livermore in the manufacture of grazing incidence X-ray telescopes, has been assessed for its applicability to manufacturing AXAF optical components. The results of that thinking indicate the expected results with respect to AXAF. These may be summarized in a series of statements as follows.

1. Precision machining, being limited to those materials compatible with the required diamond tooling, will not machine the materials that appear to have optimum properties for AXAF. - Titanium silicate, the selected material, has a yield strength above its fracture strength and thus cannot

be shear cut. This limits precision machining of glass to precision wheel grinding which, as yet, is not well enough developed to meet either figure or finish requirements established for AXAF. It may be useful as a roughing operation.

2. The typical figure and finish results of precision machining even in materials considered turnable are not nearly adequate for AXAF. - - On the latest, near state-of-the art machines, the anticipated accuracies will, at best, be: Figure - ~380Å ± ~125Å peak to valley
   Finish - ~100Å ± 254Å RMS
   Correlation lengths will be ~50 to 100 μm.

   As can be seen these will not be near good enough to meet the approximately 100Å peak to valley figure and 10 to 20Å RMS finish requirements established for AXAF. These figures indicate the precision machining will only be useful as a roughing operation.

3. A combination of precision machining and post machining lapping may well prove to be a viable approach to AXAF manufacture. - - By utilizing the high degree of geometric control offered by precision machining, the AXAF surfaces; including mounting, reference, and alignment surfaces can be rapidly generated. Then by using the dissolving lap technique described earlier, surfaces of sufficient quality may be possible. Using the metal on glass technique on strain free metals, graphite fiber composites, beryllium or other appropriate substrates, it may be possible to produce a lighter, less expensive, and more durable objective for AXAF.

Other minor efforts carried out under NASA direction as additional engineering development in the manufacture of grazing incidence X-ray optical surfaces were:

a. Several sets of scattering flats recoated with gold to serve as reference flats. - - Approximately four sets were stripped of their original coatings then vacuum coated with a chromium binder layer and finally pure gold. Considerable difficulty was encountered due to interdiffusion of the chromium into the gold which adversely effects reflectance at the soft X-ray wavelengths of interest. By switching from a chromium to a titanium binder layer the problem was eliminated.

b. A pair of coating thickness calibration samples were manufactured as a calibration on the optical heterodyne profilometer. - - These calibration samples were manufactured from chromium and consisted of a series of coated areas approximately 1.5 cm x 5.5 mm of ever increasing thickness on BK-7 substrates. The thicknesses ranged from 50Å ± 5Å to 250Å ± 5Å in 50Å steps. The thicknesses were measured using a Rank-Taylor-Hobson Talystep.

Task II - Precision Metrology for AXAF

Under the direction of Marshall Space Flight Center (MSFC), Lawrence Livermore National Laboratory provided engineering support including:

a. Measurement of 50 sets of X-ray test and scattering flats provided by MSFC. The data was to be acquired from LLNL's optical heterodyne profilometer.

b. LLNL provided MSFC time, drawings, advice and training in support of an MSFC effort to duplicate the currently existing optical heterodyne profilometer.

c. LLNL has provided MSFC with the conceptual design of several instruments to measure the axial and azimuthal profiles as well as the microtopography of grazing incidence X-ray telescopes.

II-a During the period of contract performance, LLNL has supplied, on an as required basis, data on the microtopographic character of at least 50 sets of AXAF reference scattering flats. These were tested by a combination of Nomarski Phase Contrast Microscopy and Optical Heterodyne Profilometry. Each sample surface was tested in at least two places inside the anticipated X-ray illumination footprint. An attempt was made to position the Nomarski Microphotographs at the exact location of the optical profilometer data. The data included:

a. Surface profiles around a 200 μm diameter circle;
b. RMS and peak to valley roughness measures;
c. Autocovariance plots;
d. Spectral density functions; and
e. Height and slope distributions presented in histographic form.

Results on samples from all sources indicated very high quality surfaces. The typical roughnesses were less than 20Å RMS and the correlation lengths on the order of 0.1μm. A number of samples showed coating artifacts, pits, scratches and areas where the coating adherence was low but the overall character was of high quality.

II-b Lawrence Livermore National Laboratory has supplied MSFC with all requested assistance in producing a duplicate of the optical heterodyne profilometer in Huntsville. This assistance has taken the form of advice as necessary and as many drawings, circuit diagrams, and component specifications as were available. As of this writing, the MSFC profilometer is completed and operational with the exception of some minor problems plaguing the phase measurement conversion scheme and final packaging.

II-c A major area of effort has been directed at developing instrumental concepts to measure axial and azimuthal profiles of grazing incidence X-ray telescope surfaces. This was approached primarily as a problem of extending the principle, developed in the optical heterodyne profilometer, to non-flat surfaces. A number of possible concepts based on the profilometer principle were investigated to determine their relative usefulness in providing statistics of the surface profile and microtopography.

The heterodyne profilometer consists of three basic components: a laser source, an interferometer, and electronics for reducing data (shown schematically in Figure 1). The laser source is a single mode helium-neon laser. The center frequency, with a wavelength of 0.6328 μm, is split into two beams 2 MH_z apart. Splitting is the result of the Zeeman effect where an axial magnetic field is applied to the laser's plasma tube, producing two superimposed beams linearly polarized in orthogonal directions.

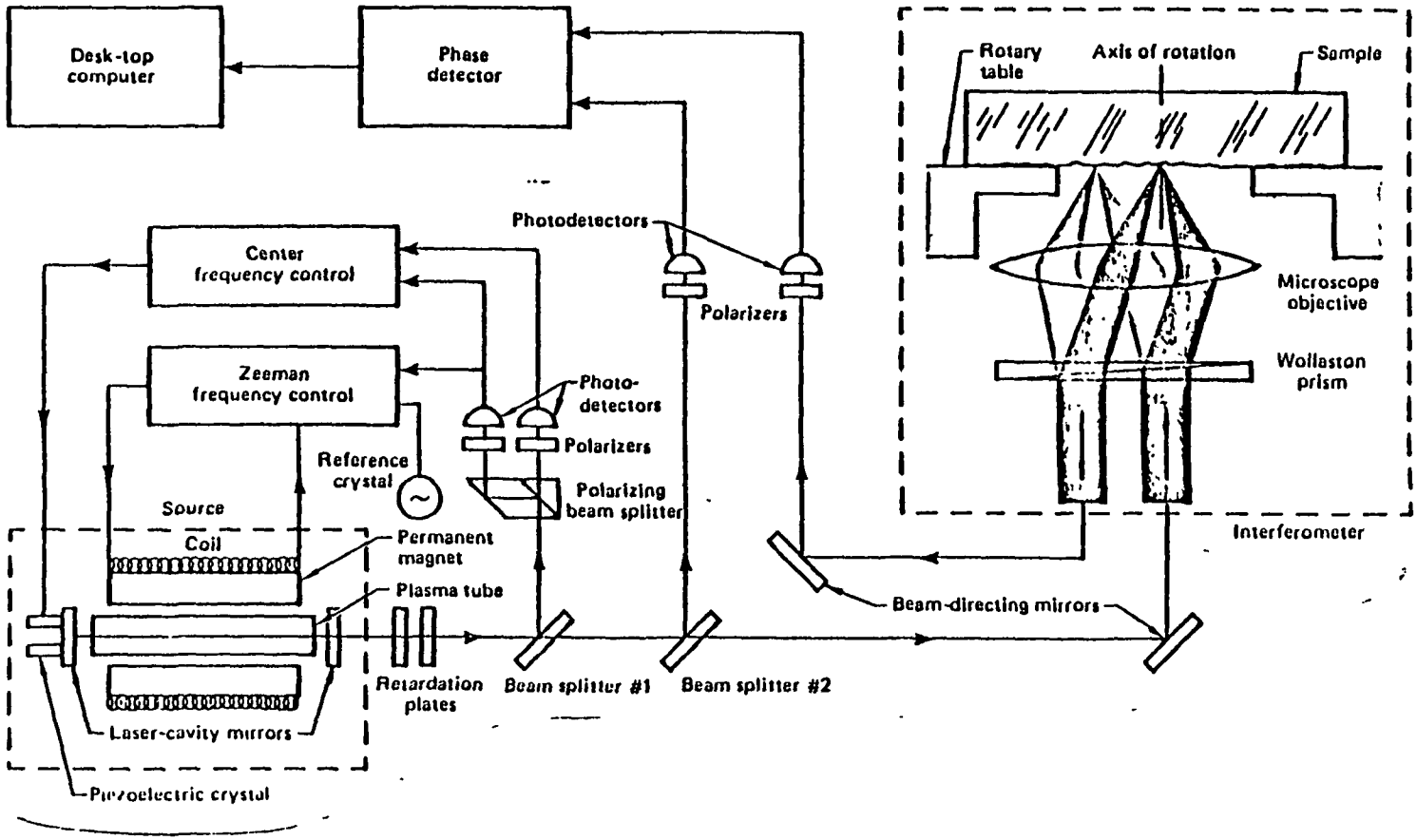

FIGURE I

Schematic diagram of the optical heterodyne profilometer

The two frequency-split, superimposed beams pass through a spatial filter/telescope that removes spatial beam noise and then through a beam splitter (#2 in Figure 1) that splits them equally. Half is directed through a polarizer rotated 45° with respect to each (superposed) beam's polarization. This causes half of each superposed beam to interfere with half the other, generating a 2 MHz beat frequency. A reference photodetector in the path of the superposed beam generates a proportionate 2 MHz signal that goes to a phase detector.

The other half of the split beam travels to the interferometer, which consists of a Wollaston polarizing prism, a microscope objective, and a precision air-bearing rotary table supporting the test surface (upper right portion of Figure 1). The polarizing prism separates the superposed beams, and the microscope objective focuses them onto the test surface. The two focal points are adjusted so that one falls exactly on the axis of the rotary table and the other 100 μm radially away.

Any physical height difference between the two focal points on the rotating test surface will produce a corresponding difference in the lengths of the paths traversed by the two separated beams. Because the height of the focal point of the axial beam is fixed, the varying height of the circular path traced about it by the second beam represents the difference in path lengths. When the reflected beams are recombined by the same optical system, any path-length difference causes a phase shift in the beat frequency. This phase shift is detected and compared with the signal from the reference detector (upper left portion of Figure 1).

As the measurement is made by detecting phase changes, the original Zeeman frequency split must be extremely stable. Otherwise, the detected phase change would result from frequency shifts in the laser beam and not from height changes in the surface as desired. We ensured stability by placing a phase-lock loop on the frequency split and on intensity analog loop on the frequency (lower left portion of Figure 1). The split frequency is identified by comparing the beat frequency between the two output beams against an external 2 MHz crystal reference. If the phase match is lost, the control system alters the axial magnetic field until the lock (correct split) is again achieved.

The center frequency is stabilized (absolute frequency) by recognizing that Zeeman splitting shifts the two beams exactly the same distance (one up and one down) from the center frequency (Figure 2a). Consequently, when the two split beams are the same, the center frequency must be exactly in the center of the gain curve and hence, fixed at the correct frequency. Were the center frequency to shift, the two beams would have different intensities (Figure 2b). The relative intensity of the beams provides an error signal that drives a piezoelectric crystal controlling the lengtn of the laser cavity, which, in turn, controls the center frequency of the laser.

The major factor in the relative usefulness of one profilometer configuration over another is the relative motion of one of the two focused spots on the surface with respect to the second, and of both spots with respect to external mechanical motions. The major method explored was the case used in the currently operating system where one spot rotates about a second fixed point. Also, two cases where both spots move with respect to the surface were explored. These are the cases where one spot follows the other

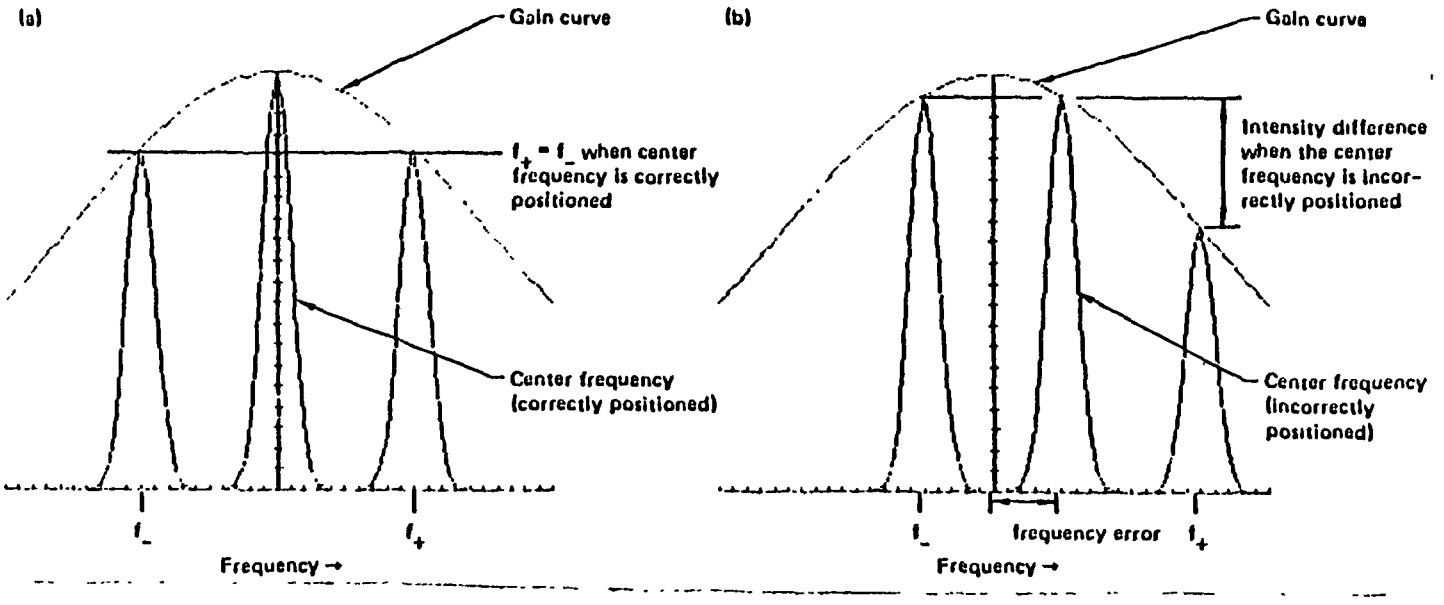

FIGURE II

Effect on Zeeman Split Lines when laser center frequency shifts

along a straight line path and a second where both spots are moved in a direction perpendicular to the line joining the spot centers. Details of the actual statistical analysis are again presented in Appendix I. The results of this work indicates that for Case 1, that it is possible to obtain the desired RMS and peak to valley values along with such statistical values as the power spectral density, the autocorrelation function and the height and slope distributions. The second case (one spot following a second) also allows achievement of reasonable values for all statistical values, but is found to be limited in terms of the spatial bandwidth that a potential system could resolve. The third case, that of two points moving parallel to one another along a direction perpendicular to the line joining their centers has been determined to be of little use in this particular application. It is possible to get some measure of one point on the autocorrelation function and estimates of such parameters as the variance and height and slope distributions. In this case, however, it is not possible to get sound estimates of the other important factors.

At this writing two concepts have been developed for the measurement of microtopography on non-flat components. The first of these utilizes the configuration where one spot follows another along a straight trace. This is applicable to X-ray components in the situation where two spots are placed on the same azimuth circle of the X-ray telescope surface and moved around the surface in a precise way. This is accomplished by rotating the X-ray telescope mirror about its axis. The second concept is one in which the two spots are configured such that one spot rotates about a second one which is fixed as in the original profilometer configuration. The difference here being that it is the optical system that is rotated rather than the test surface. It is the second configuration that is of most interest as it can be applied to any number of optical surface geometries. The only requirement is that the change in the surface height across a 200 micron diameter circle not exceed the depth of focus of the microscope objective used to form the two spots of light. Appendix 2 contains optical systematic diagrams, a block diagram of the electronic data acquisition and control system and a conceptual layout of a potential machine for making measurements on large X-ray optical surfaces. Our preliminary thinking indicates that the simpler configuration whereby the part is moved by a fixed optical system is the only practical one, due to the fact that the rotating optical head system requires an optical component of a type that we have yet to determine. Therefore, it is our recommendation that NASA pursue the simpler of these two configurations as a potential method for measuring microtopography on surfaces of this geometry. This technique may also be useful for measuring profile by simply moving the optical axially or radially against well understood (calibrated) slideways.

Acknowledgements

The principal investigator wishes to express his sincere thanks to all those who helped, aided, and participated in this program. Particular thanks go to Charles L. Wyman of MSFC who guided our efforts so ably. Thanks also go to R. T. Maney, W. E. Alston, R. Raether, P. Hed, J. W. Dini and Richard Mensing of Lawrence Livermore National Laboratory whose efforts are sincerely appreciated. Finally, the support of both NASA's George C. Marshall Space Flight Center and the Smithsonian Astrophysical Laboratory are acknowledged with gratitude.

APPENDIX I

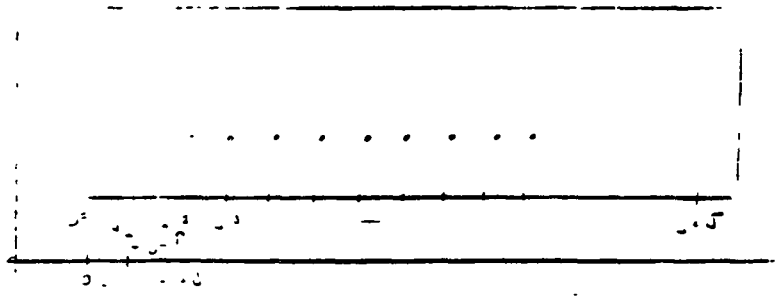

f_j = [illegible] AT j

μ_f = [illegible] SURFACE

= [illegible] CONSTANT)

σ_f^2 = VARIATION IN SURFACE RELATIVE TO f_0

(RELATIVE) VARIANCE OF TRUE SURFACE VALUES

IE FOR FIXED j, $\sigma_f^2 = \int (f_j - f_0)^2 g(f_j)\, df_j$

WHERE $g(f_j)$ IS DENSITY OF DISTRIBUTION OF TRUE SURFACE VALUES

[NOTE: ASSUMES $g(\cdot)$ IS SAME FOR ALL j]

$\alpha(\eta)$ = 'JOINT' 'RELATIVE' VARIATION IN SURFACE

'RELATIVE' COVARIANCE OF TRUE SURFACE VALUES

I.E. FOR $j \neq k$ SUCH THAT $L_k - L_j = \eta$, $\alpha(\eta) = \iint (f_j - f_0)(f_k - f_0)\, g(f_j, f_k)\, df_j$

ASSUME NO MEASUREMENT ERROR, I E. ASSUME

$$X_j = f_j$$

CONSIDER THE MEASUREMENTS

$$D_j(k) = X_{j+k} - X_j$$

THEN,

$$\begin{aligned} E[D_j(k)] &= E(f_{j+k}) - E(f_j) \\ &= 0 \end{aligned}$$

$$\begin{aligned} \mathrm{Var}[D_j(k)] &= E[(f_{j+k} - f_j)^2] \\ &= E\{[(f_{j+k} - f_0) - (f_j - f_0)]^2\} \\ &= E[(f_{j+k} - f_0)^2 - 2(f_{j+k} - f_0)(f_j - f_0) + (f_j - f_0)^2] \\ &= 2\sigma_f^2 - 2\alpha(kS) \end{aligned}$$

$$= \gamma(\delta) - \alpha[(\ell+1)\delta] - \alpha[(\ell-1)\delta]$$

UNDER THE STATISTICS

1. $$S_1(0) = \frac{1}{J}\sum_{j=1}^{J}\left[\sum_{k=1}^{j} D_k(1)\right]^2$$

$$= \frac{1}{J}\sum_{j=1}^{J}\left[\sum_{k=1}^{j}(X_{k+1} - X_k)\right]^2$$

$$= \frac{1}{J}\sum_{j=1}^{J}(X_j - X_0)^2$$

$$\mathcal{E}\left[S_1(0)\right] = \frac{1}{J}\sum_{j=1}^{J}\mathcal{E}(X_j - X_0)^2$$

$$= \frac{1}{J}\sum_{j=1}^{J} \mathrm{Var}(f_0)$$

$$= \sigma_f^2$$

2. $$S_k(\delta) = \frac{1}{2J}\sum_{j=1}^{J} D_j^2(k)$$

$$= \frac{1}{2J}\sum_{j=1}^{J}(X_{j+k} - X_j)^2$$

$$\mathcal{E}\left[S_k(\delta)\right] = \frac{1}{2J}\sum_{j=1}^{J}\mathcal{E}\left[(X_{j+k} - X_0) - (X_j - X_0)\right]^2$$

$$= \frac{1}{2J}\sum_{j=1}^{J}\mathcal{E}\left[(X_{j+k} - X_0)^2 - 2(X_{j+k} - X_0)(X_j - X_0) + (X_j - X_0)^2\right]$$

$$= \frac{1}{2J}\sum_{j=1}^{J}\left[\sigma_f^2 - 2\alpha(k\delta) + \sigma_f^2\right]$$

$$= \left[\sigma_f^2 - \alpha(k\delta)\right]$$

$$= \gamma(k\delta) - \sigma_f^2$$

$$= [(f_{j+1} - f_0) - (f_j - f_0)][(f_{j+k+1} - f_0) - (f_{j+k} - f_0)]$$

$$= (f_{j+1} - f_0)(f_{j+k+1} - f_0) - (f_j - f_0)(f_{j+k+1} - f_0) - (f_{j+1} - f_0)(f_{j+k} - f_0) + (f_j - f_0)(f_{j+k} - f_0)$$

$$= \alpha(k\delta) - \alpha[(k+1)\delta] - \alpha[(k-1)\delta]$$

CONSIDER THE STATISTICS

1. $$S_1(0) = \frac{1}{J}\sum_{j=1}^{J}\left[\sum_{k=1}^{j} D_k(1)\right]^2$$

$$= \frac{1}{J}\sum_{j=1}^{J}\left[\sum_{k=1}^{j}(X_{k+1} - X_k)\right]^2$$

$$= \frac{1}{J}\sum_{j=1}^{J}(X_j - X_0)^2$$

$$E[S_1(0)] = \frac{1}{J}\sum_{j=1}^{J} E(X_j - X_0)^2$$

$$= \frac{1}{J}\sum_{j=1}^{J} \mathrm{Var}(f_j)$$

$$= \sigma_f^2$$

2. $$S_k(\delta) = \frac{1}{2J}\sum_{j=1}^{J} D_j^2(k)$$

$$= \frac{1}{2J}\sum_{j=1}^{J}(X_{j+k} - X_j)^2$$

$$E[S_k(\delta)] = \frac{1}{2J}\sum_{j=1}^{J} E[(X_{j+k} - X_0) - (X_j - X_0)]^2$$

$$= \frac{1}{2J}\sum_{j=1}^{J} E[(X_{j+k} - X_0)^2 - 2(X_{j+k} - X_0)(X_j - X_0) + (X_j - X_0)^2]$$

$$= \frac{1}{2J}\sum_{j=1}^{J}[\sigma_f^2 - 2\alpha(k\delta) + \sigma_f^2]$$

$$= \left[\sigma_f^2 - \alpha(k\delta)\right]$$

$$D_{ij} = f_i - f_0 + E_{ij}$$

AND

$$\Delta_{ij} = D_{ij} - D_{ij+\frac{n}{2}} \qquad j = 1, \ldots \frac{n}{2}\ ;\ n = \text{NUMBER REPLICATE}$$

THEN,

$$\begin{aligned} E(\Delta_{ij}) &= E\left[D_{ij} - D_{ij+\frac{n}{2}} \right] \\ &= 0 \end{aligned}$$

$$\begin{aligned} Var(\Delta_{ij}) &= E\left[(D_{ij} - D_{ij+\frac{n}{2}})^2 \right] \\ &= E\left[\left\{ (f_i - f_0 + E_{ij}) - (f_i - f_0 + E_{ij+\frac{n}{2}}) \right\}^2 \right] \\ &= E\left[(E_{ij} - E_{ij+\frac{n}{2}})^2 \right] \\ &= 2\sigma_E^2 \end{aligned}$$

THUS, CONSIDER THE ESTIMATOR

$$S_E(0) = \frac{1}{Nn} \sum_{i=1}^{N} \sum_{j=1}^{\frac{n}{2}} \Delta_{ij}^2$$

THEN,

$$\begin{aligned} E\left(S_E(0) \right) &= \frac{1}{Nn} \sum_{i=1}^{N} \sum_{j=1}^{\frac{n}{2}} E(\Delta_{ij}^2) \\ &= \sigma_E^2 \end{aligned}$$

THUS,

$S_k(\delta)$ IS AN UNBIASED ESTIMATOR OF $\alpha(k\delta)$

$S_E(0)$ IS AN UNBIASED ESTIMATOR OF σ_E^2

$\max\left\{ S_1(0) - S_E(0)\ ;\ 0 \right\}$ IS AN ESTIMATOR OF σ_f^2

FOR THE LINEAR SCAN, THE MODEL FOR THE MEASUREMENTS IS

$$D_j(k) = f_{j+k} - f_j + E_j$$

SUCH THAT

$$E(E_j) = 0$$

$$Var(E_j) = \sigma_E^2$$

$$E(E_j E_{j'}) = 0$$

SUPPOSE WE INTRODUCE A MEASUREMENT ERROR, I.E. FOR CIRCULAR SCAN

$$D_i = f_i - f_0 + E_i$$

WHERE

$$E(E_i) = 0$$

$$Var(E_i) = \sigma_E^2$$

$$E(E_i E_{i'}) = 0$$

ALSO,

$$E(f_i E_j) = 0 \qquad \text{FOR ALL } (i, j).$$

THEN,

$$E(D_i) = 0$$

$$Var(D_i) = \sigma_f^2 + \sigma_E^2$$

$$Cov(D_i, D_{i+k}) = E(D_i D_{i+k}) = E\left[(f_i - f_0 + E_i)(f_{i+k} - f_0 + E_{i+k})\right]$$

$$= E\left[(f_i - f_0)(f_{i+k} - f_0) + E_i (f_{i+k} - f_0) + (f_i - f_0)E_{i+k} + E_i E_{i+k}\right]$$

$$= a(k\delta)$$

THUS, (CONSIDER) THE ESTIMATORS

$$S_1(0) = \frac{1}{N} \sum_{i=1}^{N} D_i^2$$

$$E\left[S_1(0)\right] = \frac{1}{N} \sum_{i=1}^{N} E(D_i^2)$$

$$= \sigma_f^2 + \sigma_E^2$$

AND

$$S_k(\delta) = \frac{1}{N} \sum_{i=1}^{N} D_i D_{i+k}$$

$$E\left[S_k(\delta)\right] = \frac{1}{N} \sum_{i=1}^{N} E(D_i D_{i+k})$$

$$= a(k\delta)$$

FOR ANY FIXED i, DEFINE

D_{ij} = jth 'REPLICATE' OF THE i-th DIFFERENCE

$\Delta t = \alpha(k\delta)$

$$\overline{I_k}(\delta) = \frac{S_k(\delta) + S_k(0)}{S_1(0)} = 1 + \frac{S_k(\delta)}{S_1(0)}$$

IS AN ESTIMATOR OF THE [illegible] CORRELATION FUNCTION

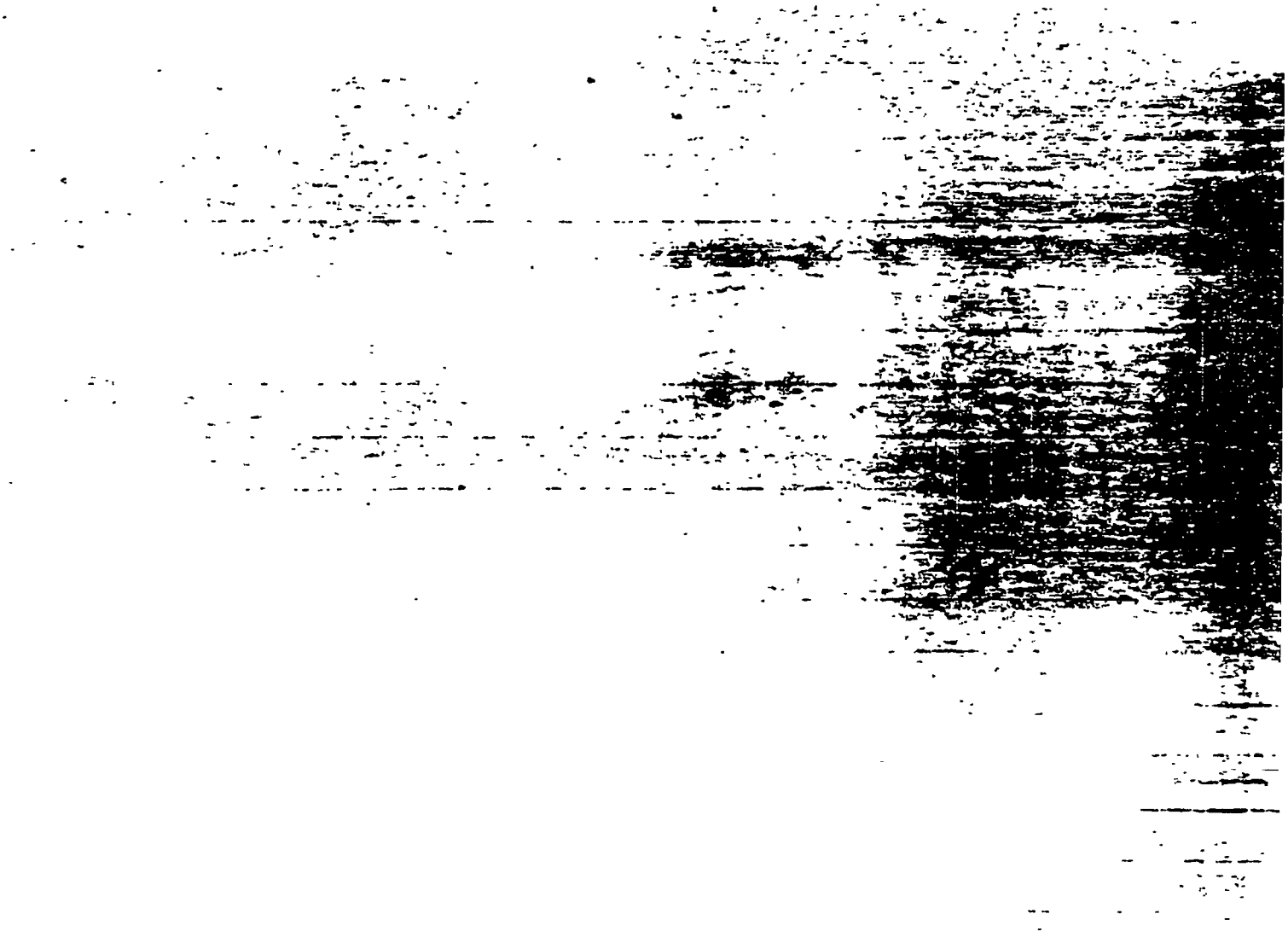

ALSO,

$$\mathcal{E}(f_j \Xi_{j'}) = 0 \qquad \text{FOR ALL } (j, j')$$

SO,

$$\mathcal{E}[D_j(k)] = 0$$

$$\begin{aligned} Var[D_j(k)] &= \mathcal{E}[D_j^2(k)] \\ &= \mathcal{E}\left[\{(f_{j+k} - f_j) + \Xi_j\}^2\right] \\ &= \mathcal{E}\left[\{(f_{j+k} - f_0) - (f_j - f_0)\}^2 + 2\Xi_j\{(f_{j+k} - f_0) - (f_j - f_0)\} + \Xi_j^2\right] \\ &= 2\sigma_f^2 - 2\rho(k\delta) + \sigma_\Xi^2 \end{aligned}$$

CONSIDER THE STATISTICS

$$1 \qquad S_1(0) = \frac{1}{J}\sum_{j=1}^{J}\left[\sum_{k=1}^{j} D_k(1)\right]^2$$

THEN,

$$\mathcal{E}[S_1(0)] = \frac{1}{J}\mathcal{E}\sum_{j=1}^{J}\left[\sum_{k=1}^{j}(f_{k+1} - f_k + \Xi_k)\right]^2$$

$$= \frac{1}{J}\mathcal{E}\sum_{j=1}^{J}\left[(f_j - f_0) + \sum_{k=1}^{j}\Xi_k\right]^2$$

$$= \frac{1}{J}\mathcal{E}\sum_{j=1}^{J}\left[(f_j - f_0)^2 + 2(f_j - f_0)\sum_{k=1}^{j}\Xi_k + \left(\sum_{k=1}^{j}\Xi_k\right)^2\right]$$

$$= \frac{1}{J}\left\{\sum_{j=1}^{J}(f_j - f_0)^2 + 2\sum_{j=1}^{J}(f_j - f_0)\sum_{k=1}^{j}\Xi_k + \sum_{j=1}^{J}\left(\sum_{k=1}^{j}\Xi_k\right)^2\right\}$$

$$= \frac{1}{J}\left\{\sum_{j=1}^{J}\mathcal{E}(f_j - f_0)^2 + 2\sum_{j=1}^{J}\mathcal{E}\left[(f_j - f_0)\sum_{k=1}^{j}\Xi_k\right] + \sum_{j=1}^{J}\mathcal{E}\left(\sum_{k=1}^{j}\Xi_k\right)^2\right\}$$

$$= \sigma_f^2 + \frac{1}{J}\sum_{j=1}^{J}\left[\sum_{k=1}^{j}\mathcal{E}(\Xi_k^2) + \sum_{k\neq k'}\mathcal{E}(\Xi_k \Xi_{k'})\right]$$

$$= \sigma_f^2 + \frac{1}{J}\sigma_\Xi^2\sum_{j=1}^{J} j$$

$$= \sigma_f^2 + \frac{J+1}{2}\sigma_\Xi^2$$

2. $\gamma_k(\delta) = -\frac{1}{2J}\sum_{j=1}^{J} D_j^2(k)$

THEN,

$$E[\gamma_k(\delta)] = -\frac{1}{2J}\,E\left\{\sum_{j=1}^{J}(f_{j+k}-f_j+\varepsilon_j)^2\right\}$$

$$= -\frac{1}{2J}\sum_{j=1}^{J} E(f_{j+k}-f_j-\varepsilon_j)^2$$

$$= -\frac{1}{2J}\sum_{j=1}^{J} E\left[(f_{j+k}-f_0)-(f_j-f_0)+\varepsilon_j\right]^2$$

$$= -\frac{1}{2J}\sum_{j=1}^{J} E\left\{(f_{j+k}-f_0)^2-2(f_{j+k}-f_0)(f_j-f_0)+(f_j-f_0)^2+2(f_{j+k}-f_0)\varepsilon_j\right.$$

$$\left.-2(f_j-f_0)\varepsilon_j+\varepsilon_j^2\right\}$$

$$= -\frac{1}{2J}\sum_{j=1}^{J}\left[\sigma_f^2-2\alpha(k\delta)+\sigma_f^2+\sigma_\varepsilon^2\right]$$

$$= \alpha(k\delta)-\sigma_f^2-\frac{1}{2}\sigma_\varepsilon^2$$

DEFINE ε_j

$D_{jl}(1)$ = l-th 'REPLICATE' OF THE 1δ BACKWARD DIFFERENCE AT j $\qquad l = 1, 2, \ldots, \frac{n}{2}$, n = NUMBER OF REPL. OF $j = 1, \ldots, J$

$$= f_{j+1} - f_j + \varepsilon_{jl}$$

AND

$$\Delta_{jl} = D_{jl}(1) - D_{j,l+\frac{n}{2}}(1)$$

THEN,

$$E(\Delta_{jl}) = E\left\{D_{jl}(1) - D_{j,l+\frac{n}{2}}(1)\right\} = 0$$

$$\mathrm{Var}(\Delta_{jl}) = E\left\{(D_{jl}(1) - D_{j,l+\frac{n}{2}}(1)\right\}^2$$

$$= E\left\{(f_{j+1}-f_j+\varepsilon_{jl})-(f_{j+1}-f_j+\varepsilon_{j,l+\frac{n}{2}})\right\}^2$$

$$= E\left\{\left[E_{j\ell} - E_{j\,\ell+\frac{n}{2}}\right]^2\right\}$$

$$= 2\sigma_E^2$$

CONSIDER THE ESTIMATOR

$$S_E = \frac{1}{Jn}\sum_{j=1}^{J}\sum_{\ell=1}^{n/2}\Delta_{j\ell}^2$$

$$= \frac{1}{Jn}\sum_{j=1}^{J}\sum_{\ell=1}^{n/2}\left\{D_{j\ell}(1) - D_{j\,\ell+\frac{n}{2}}(1)\right\}^2$$

THEN,

$$E(S_E) = \sigma_E^2$$

SO S_E IS AN UNBIASED ESTIMATOR OF σ_E^2.

THUS

S_E IS AN UNBIASED ESTIMATOR OF σ_E^2

$S_f \equiv \min\left\{S_1(0) - \frac{J+1}{2}S_E,\ 0\right\}$ IS AN ESTIMATOR OF σ_f^2

$S_\alpha = S_k(\delta) + S_1(0) + \frac{1}{2}S_E$ IS AN ESTIMATOR OF $\alpha(2\delta)$

...F A NON-CONTACT OPTICAL ...

...HNIQUE FOR THE MEASUREMENT OF SURFACE PROFILE

FIXED CENTER POINT, CIRCULAR SCAN

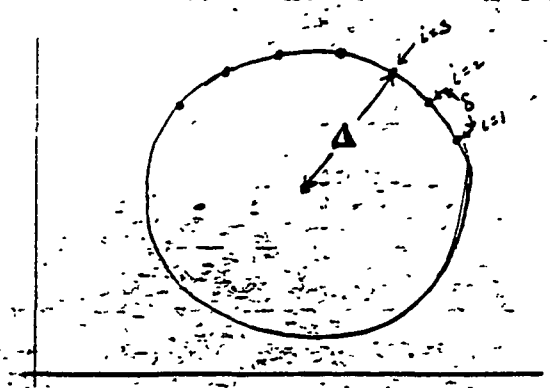

LET X_i – SURFACE MEASUREMENT AT i

X_0 – SURFACE MEASUREMENT AT CENTER POINT

f_i – TRUE SURFACE VALUE AT i

μ_{f_i} – 'DESIGNED' SURFACE
$\equiv 0$ (ASSUMED TO BE CONSTANT)

$\sigma_f^2 \equiv$ VARIATION IN SURFACE (RELATIVE TO f_0)
DESCRIBED BY VARIANCE OF TRUE SURFACE VALUES

$\alpha(\eta) \equiv$ 'JOINT' VARIATION IN SURFACE
DESCRIBED BY AUTOCOVARIANCE OF TRUE SURFACE VALUES

ASSUME NO MEASUREMENT ERROR, I.E. ASSUME

$$X_i \equiv f_i$$

SO THAT ANY VARIATION IN X_i IS REFLECTION OF VARIATION IN SURFACE.

FOR CIRCULAR SCAN, THE REALIZED MEASUREMENT IS

$$D_i = X_i - f_0$$

ASSUME

$$f_0 = \mu_{f_0} = 0$$

I.E. ALL MEASUREMENTS TAKEN RELATIVE TO SURFACE VALUE AT CENTER POINT NOTE: IF $f_0 \neq 0$ A BIAS IS INTRODUCED. UNDER THE ASSUMPTION,

$$E(D_i) = E(X_i)$$

$$= \mu_{f_i} = 0$$

$$Var(D_i) = Var(X_i - f_0) \equiv \sigma_i^2$$

$$Cov(D_i, D_{i+k}) = E(D_i D_{i+k}) = E[(X_i - f_0)(X_{i+k} - f_0)]$$

$$\equiv \alpha(k\delta)$$

$$E[S_1(0)] = \frac{1}{2I}\sum_{i=1}^{I} E\left[(X_{iJ} - X_{i1})^2\right]$$

$$= \frac{1}{2I}\sum_{i=1}^{I} E\left[X_{iJ}^2 - 2X_{i1}X_{iJ} + X_{i1}^2\right]$$

$$= \frac{1}{2I}\sum_{i=1}^{I} E\left[f_{iJ}^2 - 2f_{i1}f_{iJ} + f_{i1}^2\right]$$

$$= \frac{1}{2I}\sum_{i=1}^{I}\left[\sigma_f^2 - 2\alpha(J\delta) + \sigma_f^2\right]$$

$$= \sigma_f^2 - \alpha(J\delta)$$

IF J IS LARGE, CAN ASSUME $\alpha(J\delta) \doteq 0$, THUS

$$E[S_1(0)] \doteq \sigma_f^2$$

THUS $S_1(0)$ IS AN ESTIMATOR OF σ_f^2

2. $$S_k(\delta) = \frac{1}{I(J-1)}\sum_{i=1}^{I}\sum_{j=1}^{J-1} D_{ij}^2(k)$$

$$E[S_k(\delta)] = \frac{1}{2I(J-1)}\sum_{i=1}^{I}\sum_{j=1}^{J} E\left[D_{ij}^2(k)\right]$$

$$= \frac{1}{2I(J-1)}\sum_{i=1}^{I}\sum_{j=1}^{J} E\left[X_{i,j+k} - X_{ij}\right]^2$$

$$= \frac{1}{2I(J-1)}\sum_{i=1}^{I}\sum_{j=1}^{J} E\left(f_{i,j+k} - f_{ij}\right)^2$$

$$= \frac{1}{2I(J-1)}\sum_{i=1}^{I}\sum_{j=1}^{J} E\left(f_{i,j+k}^2 - 2f_{ij}f_{i,j+k} + f_{ij}^2\right)$$

$$= \frac{1}{2I(J-1)}\sum_{i=1}^{I}\sum_{j=1}^{J}\left[\sigma_f^2 - 2\alpha(k\delta) + \sigma_f^2\right]$$

$$= \alpha(k\delta) - \sigma_f^2$$

THUS $S_k(\delta) + S_1(0)$ IS AN ESTIMATOR OF $\alpha(k\delta)$, THE AUTOCOVARIANCE FUNCTION, AND

$$r_k(\delta) = \frac{S_k(\delta) + S_1(0)}{S_1(0)} = 1 + \frac{S_k(\delta)}{S_1(0)}$$

IS AN ESTIMATOR OF THE AUTOCORRELATION FUNCTION

NO FIXED POINT, LINEAR SCAN

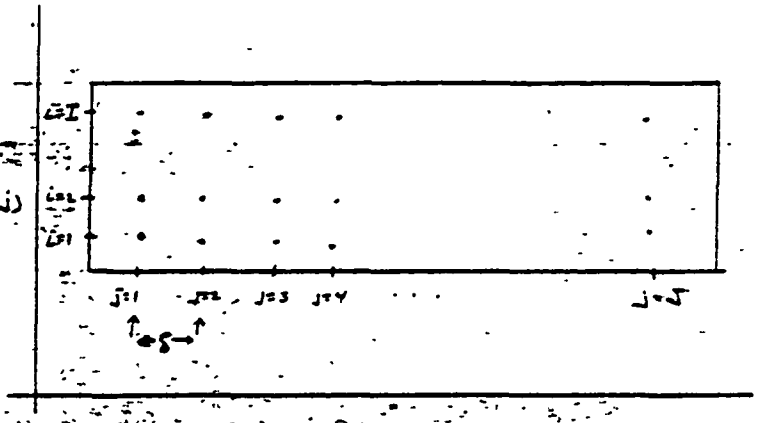

LET X_{ij} = SURFACE MEASUREMENT AT (i,j)

f_{ij} = TRUE SURFACE VALUE AT (i,j)

$\mu_{f_{ij}}$ = 'DESIGNED' SURFACE $\equiv 0$ (ASSUMED CONSTANT)

σ_f^2 = VARIATION IN SURFACE
VARIANCE OF TRUE SURFACE VALUES

$\alpha(\eta)$ = 'JOINT' VARIATION IN SURFACE
COVARIANCE OF TRUE SURFACE VALUES

ASSUME NO MEASUREMENT ERROR, I.E. ASSUME

$$X_{ij} = f_{ij}$$

CONSIDER THE MEASUREMENTS

$$D_{ij}(k) = X_{ij+k} - X_{ij}$$

THEN,

$$\mathcal{E}[D_{ij}(k)] = \mathcal{E}(f_{ij+k}) - \mathcal{E}(f_{ij})$$
$$= 0$$

$$\mathrm{Var}[D_{ij}(k)] = \mathcal{E}\left[f_{ij+k} - f_{ij}\right]^2$$
$$= \mathcal{E}(f_{ij+k}^2) - 2\mathcal{E}(f_{ij+k} f_{ij}) + \mathcal{E}(f_{ij}^2)$$
$$= 2\sigma_f^2 - 2\alpha(k\delta)$$

$$\mathrm{Cov}\left[D_{ij}(l), D_{ij+l}(l)\right] = \mathcal{E}\left[(f_{ij+l} - f_{ij})(f_{ij+2l} - f_{ij+l})\right]$$
$$= \mathcal{E}(f_{ij+l} f_{ij+2l}) - \mathcal{E}(f_{ij} f_{ij+2l}) - \mathcal{E}(f_{ij+l} f_{ij+l}) + \mathcal{E}(f_{ij} f_{ij+l})$$
$$= 2\alpha(l\delta) - \alpha[(l+1)\delta] - \alpha[(l-1)\delta]$$

CONSIDER THE STATISTIC

$$S_1(0) = \frac{1}{2I}\sum_{i=1}^{I}\left[\sum_{j=1}^{J} D_{ij}(1)\right]^2 = \frac{1}{2I}\sum_{i=1}^{I}\left[\sum_{j=1}^{J}(X_{ij+1} - X_{ij})\right]^2 = \frac{1}{2I}\sum_{i=1}^{I}(X_{iJ} - X_{i1})^2$$

AS AN ALTERNATIVE, CONSIDER THE ESTIMATOR

$$S_1^*(0) = \frac{1}{2I(J-L)} \sum_{i=1}^{I} \sum_{l=L+1}^{J} \left[\sum_{j=1}^{L} D_{ij}(l) \right]^2$$

$$= \frac{1}{2I(J-L)} \sum_{i=1}^{I} \sum_{l=L+1}^{J} \left[\sum_{j=1}^{L} (X_{i,j+l} - X_{ij}) \right]^2$$

$$= \frac{1}{2I(J-L)} \sum_{i=1}^{I} \sum_{l=L+1}^{J} (X_{il} - X_{ij})^2$$

(L large)

$$E[S_1^*(0)] = \frac{1}{2I(J-L)} \sum_{i=1}^{I} \sum_{l=L+1}^{J} E(X_{il} - X_{ij})^2$$

$$= \frac{1}{2I(J-L)} \sum_{i=1}^{I} \sum_{l=L+1}^{J} E[X_{il}$$

$$= \frac{1}{2I(J-L)} \sum_{i=1}^{I} \sum_{l=L+1}^{J} E[f_{il}$$

$$= \sigma_f^2 \; \gamma(l\delta)$$

AGAIN, IF l large, CAN ASSUME $\alpha(l\delta) \doteq 0$, THUS

$$E[S_1(0)] \doteq \sigma_f^2$$

AND $S_1(0)$ IS AN ESTIMATOR OF σ_f^2

NOTE: IF THE LENGTH OF THE SURFACE IS LARGE RELATIVE TO THE 'LAG' OF THE JOINT VARIATION IN SURFACE, COULD ESTIMATE BOTH σ_f^2 AND $\alpha(=\delta)$ BASED ON A SINGLE (IE $L=1$) LINEAR SCAN.

SUPPOSE THE OBSERVED MEASUREMENT ERROR, E_i

$$D_i \equiv X_i - f_0 = f_i - f_0 + E_i = \Delta_i + E_i$$

SUCH THAT

$$E(E_i) = 0$$

$$Var(E_i) = \sigma_M^2$$

AN ESTIMATE OF σ_M^2 IS BASED ON REPEATED MEASUREMENTS OF D_i FOR AN i, LET

$$D_{ik} \quad k = 1, \ldots N$$

DENOTE k REPETITIONS. THUS,

$$E(D_{ik}) = E\left[E(D_{ik} \mid f_i, f_0)\right]$$

$$= E[f_i - f_0]$$

$$= 0$$

$$Var(D_{ik}) = Var\left[E(D_{ik} \mid f_i, f_0)\right] + E\left[Var(D_{ik} \mid f_i, f_0)\right]$$

$$= \sigma_f^2 + \sigma_M^2$$

$$Cov(D_{ik}, D_{i,k+k'}) = E\left[Cov(D_{ik}, D_{i,k+k'} \mid f_i, f_0)\right]$$

CONSIDER, FOR $k = 0, 1, 2, \ldots$

$$\Delta_{ik} = D_{i,2(k+1)} - D_{i,2k+1}$$

$$E(\Delta_{ik}) = 0$$

$$Var(\Delta_{ik}) = Var\left[E(D_{i,2(k+1)} - D_{i,2k+1} \mid f_i, f_0)\right] + E_i\left[Var(\Delta_{ik} \mid f_i)\right]$$

$$= E\left\{Var\left[(f_i - f_0 + E_{i,2(k+1)}) - (f_i - f_0 + E_{i,2k+1}) \mid f_i, f_0\right]\right\}$$

$$= E\left\{Var(E_{i,2(k+1)} - E_{i,2k+1})\right\}$$

$$= 2\sigma_M^2$$

THUS AN UNBIASED ESTIMATOR OF σ_M^2 IS

$$s_M^2 \equiv \frac{1}{2\left[\frac{N}{2} - 1\right]} \sum_{k=1}^{\frac{N}{2}-1} (\Delta_{ik} - \bar{\Delta}_{i\cdot})^2$$

CONSIDER THE STATISTICS

$$S_1(0) = \frac{1}{N}\sum_{i=1}^{N} D_i^2$$

$$\begin{aligned} \mathcal{E}[S_1(0)] &= \frac{1}{N}\sum_{i=1}^{N} \mathcal{E}(D_i^2) \\ &= \frac{1}{N}\sum_{i=1}^{N} \mathcal{E}[(X_i - f_0)^2] \\ &= \frac{1}{N}\sum_{i=1}^{N} \sigma_f^2 \\ &= \sigma_f^2 \end{aligned}$$

IS AN ESTIMATOR OF σ_f^2

$$S_k(\delta) = \frac{1}{N}\sum_{i=1}^{N} D_i D_{i+k} \qquad k = 1, 2$$

$$\begin{aligned} \mathcal{E}[S_k(\delta)] &= \frac{1}{N}\sum \\ &= \frac{1}{N}\sum_{i=1}^{N} \mathcal{E}[(X_i - f_0)(X_{i+k} - f_0)] \\ &= \frac{1}{N}\sum_{i=1}^{N} C_{ff}(k\delta) \\ &= a(k\delta) \end{aligned}$$

IS AN ESTIMATOR OF THE AUTOCOVARIANCE FUNCTION

THUS,

$$T_k(\delta) = S_k(\delta)/S_1(0)$$

IS AN ESTIMATOR OF THE AUTOCORRELATION FUNCTION

APPENDIX II

2-15-82

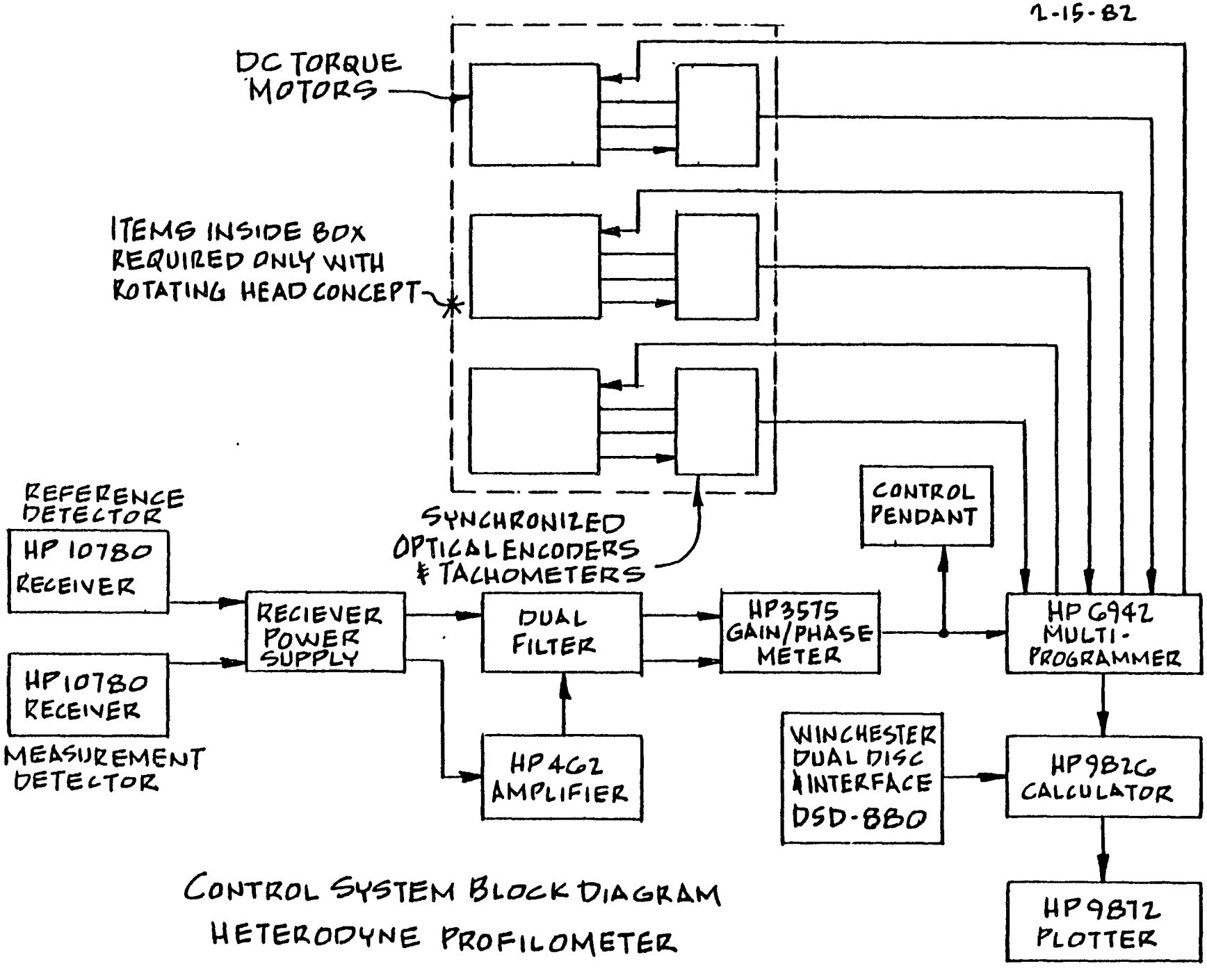

CONTROL SYSTEM BLOCK DIAGRAM
HETERODYNE PROFILOMETER

2-15-82

MOVING PART PROFILOMETER
(SYSTEM CONCEPT DIAGRAM)

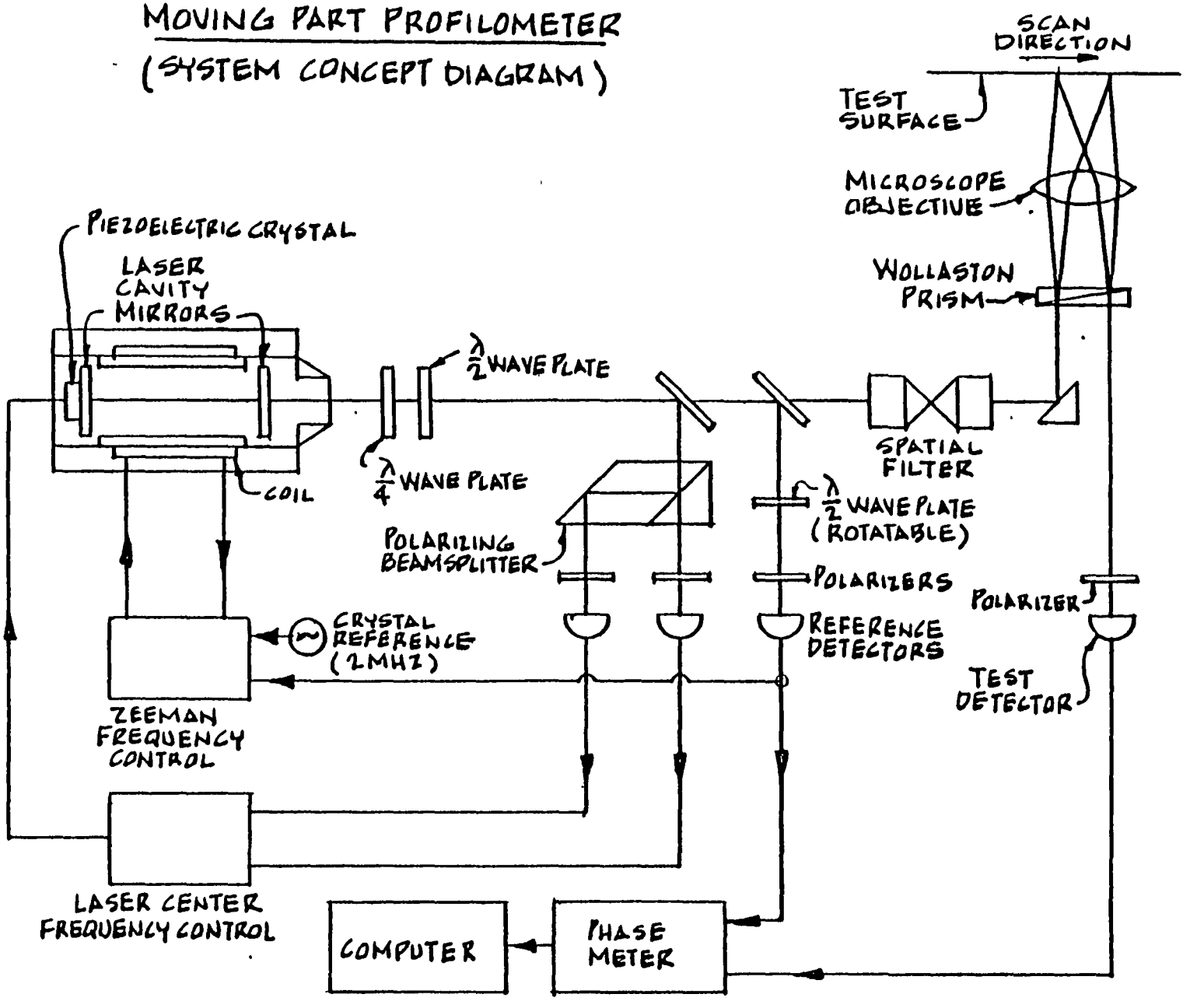

ROTATING HEAD PROFILOMETER (SYSTEM CONCEPT DIAGRAM)

NOTE 1 - DEVICE NEEDS TO BE DEVELOPED HERE THAT WILL PREVENT RETURN LIGHT FROM ENTERING THE LASER CAVITY WITHOUT ALTERING OUTWARD PROPAGATING BEAM.

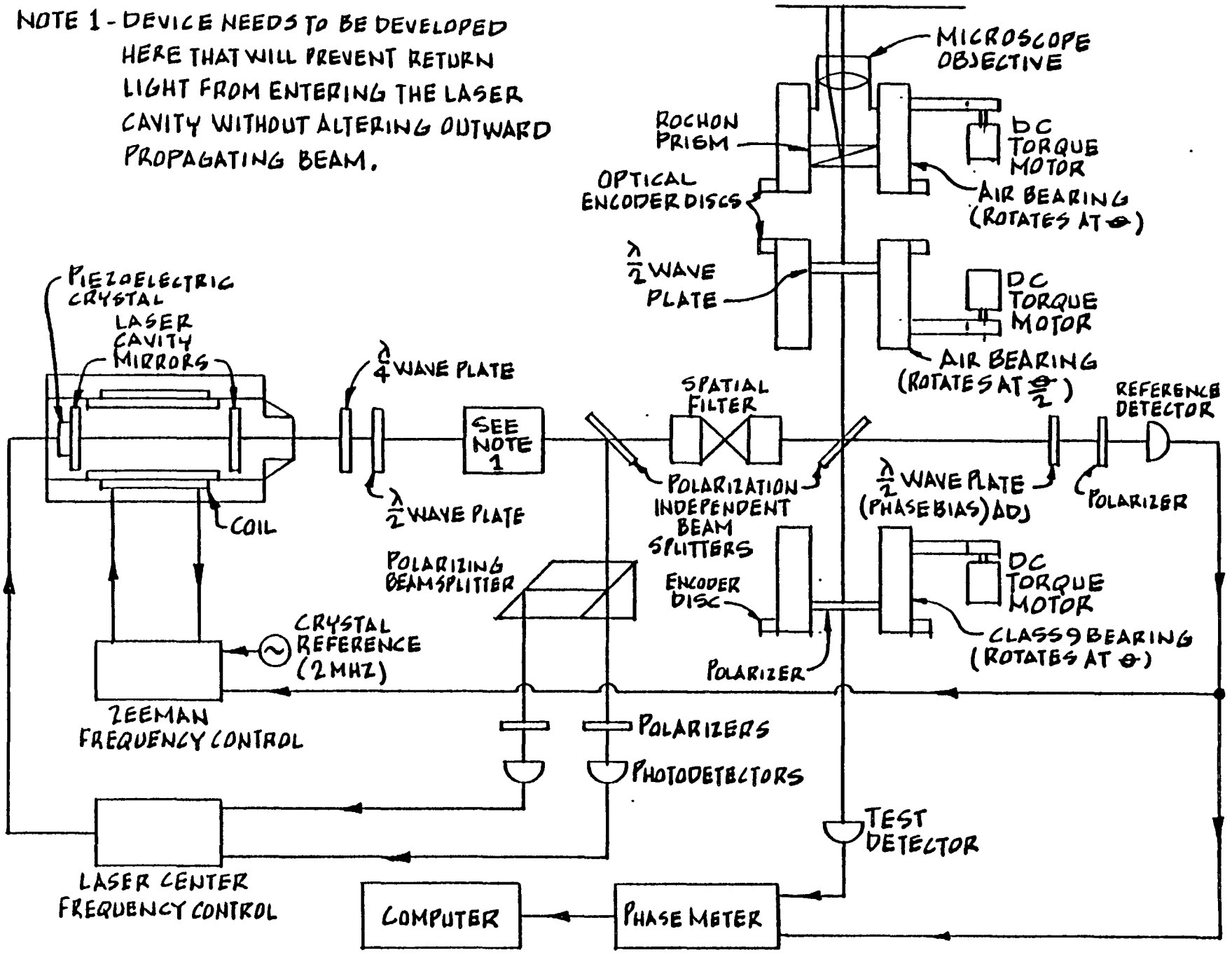

NOTES :
1. ALL STAGES MUST HAVE A POSITIONAL STABILITY OF ±0.05 μm DURING 60 MINUTES
2. CENTERING STAGES POSITIONAL RESOLUTION ±0.03 μm.
ROTARY STAGE RADIAL RUNOUT ±0.03 μm.